Inorganic Chemistry

Article

Electrochemistry, Spectroelectrochemistry, Chloride Binding, and O$_2$ Catalytic Reactions of Free-Base Porphyrin–Cobalt Corrole Dyads

Karl M. Kadish,*,† Jianguo Shao,† Zhongping Ou,† Laurent Frémond,† Riqiang Zhan,† Fabien Burdet,‡ Jean-Michel Barbe,‡ Claude P. Gros,‡ and Roger Guilard*,‡

University of Houston, Department of Chemistry, Houston, Texas 77204-5003, and Université de Bourgogne, LIMSAG UMR 5633, Faculté des Sciences Gabriel, 6 Boulevard Gabriel, 21000 Dijon, France

Three face-to-face linked porphyrin–corrole dyads were investigated as to their electrochemistry, spectroelectro-chemistry, and chloride-binding properties in dichloromethane or benzonitrile. The same three compounds were also investigated as to their ability to catalyze the electroreduction of dioxygen in aqueous 1 M HClO$_4$ or HCl when adsorbed on a graphite electrode. The characterized compounds are represented as (PCY)H$_2$Co, where P = a porphyrin dianion; C = a corrole trianion; and Y = a biphenylenyl, 9,9-dimethylxanthenyl, or anthracenyl spacer, which links the two macrocycles in a face-to-face arrangement. An axial binding of one or two Cl$^-$ ligands to the cobalt center of the corrole is observed for singly and doubly oxidized (PCY)H$_2$Co, with the exact stoichiometry of the reaction depending upon the spacer size and the concentration of Cl$^-$ added to solution. No Cl$^-$ binding occurs for the neutral or reduced forms of the dyad, which contrasts with what is seen for the monocorrole, (Me$_4$-Ph$_5$Cor)Co, where a single Cl$^-$ ligand is added to the Co(III) corrole in PhCN. The Co(III) form of the corrole in (PCY)H$_2$Co also appears to be the catalytically active species in the electroreduction of dioxygen, which occurs at potentials associated with the Co(IV)/Co(III) reaction, that is, 0.35 V in 1 M HClO$_4$ as compared to 0.31–0.42 V for the same three dyads in PhCN and 0.1 M TBAP. The potential for the catalytic electroreduction of O$_2$ in HCl shifts negatively by 60 to 70 mV as compared to $E_{1/2}$ values in 1 M HClO$_4$, consistent with the binding of Cl$^-$ to the Co(IV) form of the corrole and its rapid dissociation after electroreduction to Co(III) at the electrode surface.

Introduction

In previous studies, we have examined the electrochemistry and axial ligand binding ability of cobalt(III) corroles both in their monomeric form[1–3] and as part of a face-to-face linked dyad with a second metallomacrocycle, either another cobalt(III) corrole in the case of biscorroles[4,5] or a Co(II),[5,6] Fe(III),[7] or Mn(III)[7] porphyrin in the case of porphyrin–

corrole dyads. We have also examined the use of face-to-face bisCo(III) corroles or dyads containing one Co(III) corrole and one Co(II) porphyrin as catalysts in the elec-troreduction of O$_2$ when adsorbed on a graphite electrode in acid media.[8]

This present paper expands upon our earlier electrochemi-cal and spectroelectrochemical studies in several respects. For one, we here changed the examined species from a

---

* To whom correspondence should be addressed. E-mail: kkadish@uh.edu (K.K.); Roger.Guilard@u-bourgogne.fr (R.G.).
† University of Houston.
‡ Université de Bourgogne.
 (1) (a) Guilard, R.; Barbe, J.-M.; Stern, C.; Kadish, K. M. In *The Porphyrin Handbook*; Kadish, K. M., Smith, K. M., Guilard, R., Eds.; Elsevier: New York, 2003; Vol. 18, pp 303–349. (b) Erben, C.; Will, S.; Kadish, K. M. In *The Porphyrin Handbook*; Kadish, K. M., Smith, K. M., Guilard. R., Eds.; Academic Press: San Diego, CA, 2000; Vol. 2, pp 233–300.
 (2) Guilard, R.; Gros, C. P.; Bolze, F.; Jérôme, F.; Ou, Z.; Shao, J.; Fischer, J.; Weiss, R.; Kadish, K. M. *Inorg. Chem.* **2001**, *40*, 4845–4855.
 (3) Kadish, K. M.; Shao, J.; Ou, Z.; Gros, C. P.; Bolze, F.; Barbe, J.-M.; Guilard, R. *Inorg. Chem.* **2003**, *42*, 4062–4070.

 (4) Guilard, R.; Jérôme, F.; Barbe, J.-M.; Gros, C. P.; Ou, Z.; Shao, J.; Fischer, J.; Weiss, R.; Kadish, K. M. *Inorg. Chem.* **2001**, *40*, 4856–4865.
 (5) Kadish, K. M.; Ou, Z.; Shao, J.; Gros, C. P.; Barbe, J.-M.; Jérôme, F.; Bolze, F.; Burdet, F.; Guilard, R. *Inorg. Chem.* **2002**, *41*, 3990–4005.
 (6) Guilard, R.; Jérôme, F.; Gros, C. P.; Barbe, J.-M.; Ou, Z.; Shao, J.; Kadish, K. M. *C. R. Acad. Sci., Ser. IIc: Chim.* **2001**, *4*, 245–254.
 (7) Guilard, R.; Burdet, F.; Barbe, J.-M.; Gros, C. P.; Espinosa, E.; Shao, J.; Ou, Z.; Zhan, R.; Kadish, K. M. *Inorg. Chem.* **2005**, *44*, 3972–3983.
 (8) Kadish, K. M.; Frémond, L.; Ou, Z.; Shao, J.; Shi, C.; Anson, F. C.; Burdet, F.; Gros, C. P.; Barbe, J.-M.; Guilard, R. *J. Am. Chem. Soc.* **2005**, *127*, 5625–5631.

Chart 1

(Me₄Ph₅Cor)Co

(Et₂Me₆PhPor)H₂

(PCY)H₂Co

Y =

A   **X**   **B**
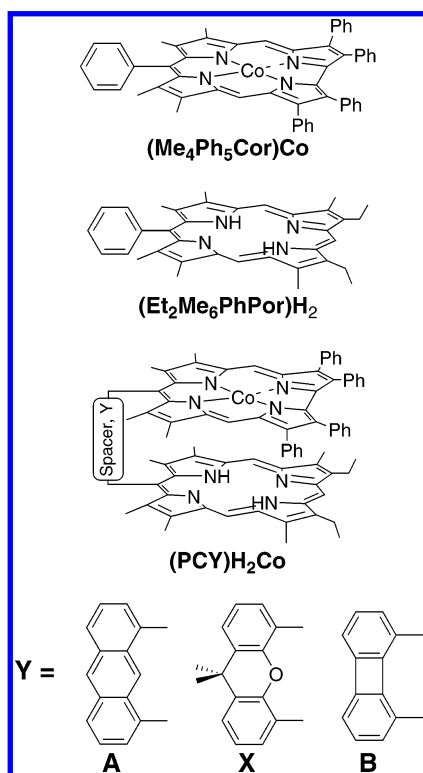
biscobalt complex with two corrole macrocycles[4,5] or one corrole and one porphyrin macrocycle[5,6,8] to a series of face-to-face linked dyads where one macrocycle is a cobalt(III) corrole and the other a free-base porphyrin.[9,10] This "removal" of a second cobalt center greatly simplifies the prevailing redox behavior and leads to a clearer understanding of how the electron-transfer and chloride-binding reactions of these face-to-face dyads are influenced in nonaqueous media by the type of spacer, size of the cavity, and solution conditions. We recently demonstrated[7] that the Co(IV) form of corrole dyads linked in a face-to-face arrangement with Mn(III) or Fe(III) porphyrins could be stabilized in a high oxidation state by the binding of Cl⁻, and the current study now presents quantitative data on the binding of Cl⁻ to both the Co(IV) and Co(III) forms of the related monocorrole as well as to three free-base porphyrin−Co(III) corrole dyads having the two macrocycles in a face-to-face orientation. We have also measured the ability of the same three dyads to catalyze the electroreduction of dioxygen in 1 M HClO₄ or 1 M HCl when adsorbed on a graphite electrode, and these results are compared to what has been reported for a series of biscobalt porphyrin−corrole dyads[8] with the same linker groups. The examined compounds are illustrated in Chart 1 and are represented as (PCY)H₂Co, where P = a porphyrin dianion; C = a corrole trianion; and Y is a biphenylenyl (B), 9,9-dimethylxanthenyl (X), or anthracenyl (A) spacer, which links the two macrocycles.

Several face-to-face bis macrocycles with one cobalt porphyrin and one free-base porphyrin have been examined as to their efficiency in the electrocatalysis of O_2 when adsorbed on an electrode surface in acid media.[11,12] These monocobalt bisporphyrins exhibit four electron reduction pathways, as evidenced by n_{app} values much greater than 2.0, and it was, therefore, of interest to examine the three (PCY)-H₂Co dyads' reactivities toward O_2 electroreduction in 1 M HClO₄ as well in 1 M HCl where Cl⁻ anions were expected, on the basis of previous studies,[7] to bind to the Co(IV) and maybe Co(III) forms of the complex.

Studies of Cl⁻ binding to the (PCY)H₂Co dyads in nonaqueous media were especially of interest since hetero-bimetallic dyads containing Co^{IV} corroles were isolated in the case of $(PCY)M^{III}ClCo^{IV}Cl$, where M = Fe or Mn[7] and some of the compounds could be converted to bischloride Co(IV) derivatives in the presence of excess Cl⁻. Especially of importance, in this regard, is the fact that the binding of Cl⁻ to the metal centers of $(TPP)Co^{II}$ and $(TPP)Co^{III}Cl$ leads to substantially easier oxidations than observed for the same species in the presence of coordinated perchlorate anions,[13−15] which is often added to solutions as a supporting electrolyte when doing electrochemistry in nonaqueous media. Thus, an additional goal of this study was to quantitatively measure the changes in $E_{1/2}$ for electrooxidation of $(PCY)H_2Co^{III}$ to its Co(IV) form since these data might prove useful in the synthesis or electrosynthesis of new Co(IV) corroles as well as provide information as to how the chemical reactivity of the chloride-containing (PCY)H₂Co dyads would change as a function of the type of bridge (A, X, and B), cobalt corrole oxidation state, and number of axially coordinated chloride ligands.

Experimental Section

Instrumentation. Cyclic voltammetry was carried out with an EG&G model 173 potentiostat. A three-electrode system was used and consisted of a glassy carbon or platinum disk working electrode, a platinum wire counter electrode, and a saturated calomel reference electrode (SCE). The SCE electrode was separated from the bulk of the solution by a fritted-glass bridge of low porosity, which contained the solvent/supporting electrolyte mixture. Half-wave potentials were calculated as $E_{1/2} = (E_{pa} + E_{pc})/2$ and are referenced to SCE.

Rotating disk experiments were carried out using a Pine model AFMSR rotator linked to an EG&G Princeton Applied Research (PAR) model 263A potentiostat/galvanostat. The potentiostat was monitored by an IBM-compatible PC microcomputer controlled by the software M270 (EG&G PARC). An RDE4 bipotentiostat (Pine Instrument) was employed with an HP 7090A three-channel digital plotter for rotating ring-disk electrode experiments. The rotating ring-disk electrode, purchased from the Pine Instrument Co.,

(9) Barbe, J.-M.; Stern, C.; Pacholska, E.; Espinosa, E.; Guilard, R. *J. Porphyrins Phthalocyanines* **2004**, *8*, 301−312.
(10) Barbe, J.-M.; Burdet, F.; Espinosa, E.; Gros, C. P.; Guilard, R. *J. Porphyrins Phthalocyanines* **2003**, *7*, 365−374.
(11) Durand, R. R.; Bencosme, S. C.; Collman, J. P.; Anson, F. C. *J. Am. Chem. Soc.* **1993**, *105*, 2710−2718.
(12) Liu, H.-Y.; Abdalmuhdi, I.; Chang, C. K.; Anson, F. C. *J. Phys. Chem.* **1985**, *89*, 665−670.
(13) Huet, J.; Gaudemer, A.; Boucly-Goester, C.; Boucly, P. *Inorg. Chem.* **1982**, *21*, 3413−3419.
(14) Kadish, K. M.; Lin, X. Q.; Han, B. C. *Inorg. Chem.* **1987**, *26*, 4161−4167.
(15) Constant, L. A.; Davis, D. G. *Anal. Chem.* **1975**, *47*, 2253−2260.

Table 1. Half-Wave Potentials (V vs SCE) for Porphyrin–Corrole Dyads, (PCY)H$_2$Co in Nonaqueous Media Containing 0.1 M TBAP

compound	solvent	oxidation					reduction			
		porphyrin		corrole			corrole		porphyrin	
(Me$_4$Ph$_5$Cor)Co[a]	PhCN			1.45[b]	0.72	0.47	−0.16	−1.67		
(Et$_2$Me$_6$PhPor)H$_2$		1.06[b]	0.92[b]						−1.42	−1.79
(PCA)H$_2$Co			1.22[b]		0.72	(**0.42**, **0.32**)[c]	−0.26	−1.67	−1.41	−1.77
(PCX)H$_2$Co			0.85		0.65	(**0.41**, **0.31**)[c]	−0.38	−1.55	−1.41	−1.73
(PCB)H$_2$Co		1.09	0.83		0.69	0.40	−0.37	−1.59	−1.41	−1.88[b]
(Me$_4$Ph$_5$Cor)Co[a]	CH$_2$Cl$_2$			1.26	0.87	(**0.62**, **0.45**)[c]	−0.15	−1.69		
(Et$_2$Me$_6$PhPor)H$_2$		1.08[b]	0.90[b]						−1.39	−1.84[b]
(PCA)H$_2$Co			1.22[b]		0.74	(**0.41**, **0.26**)[c]	−0.20	−1.74[b]	−1.42	
(PCX)H$_2$Co			0.87		0.68	(**0.41**, **0.24**)[c]	−0.39	−1.62[b]	−1.44[b]	−1.80[b]
(PCB)H$_2$Co		1.10	0.87		0.71	0.39	−0.38	−1.74[b]	−1.41	−1.74[b]

[a] Ref 3. [b] Peak potential at a scan rate of 0.1 V/s. [c] Potentials in parentheses correspond to oxidations of a dimer formed between two dyads in solution.

consisted of a platinum ring and a removable edge-plane pyrolytic graphite disk ($A = 0.282$ cm^2).

UV–visible spectroelectrochemical experiments were performed with an optically transparent platinum thin-layer electrode whose construction is described in the literature.[16] Potentials were applied with an EG&G model 173 potentiostat. Time-resolved UV–visible spectra were recorded with a Hewlett-Packard model 8453 diode array rapid-scanning spectrophotometer. UV–visible spectra of the neutral complexes were taken with the HP model 8453 spectrophotometer or with a Varian Cary 50 spectrophotometer.

Electrode Surface Preparation for O$_2$ Catalysis. Before use, the graphite disk was polished separately from the platinum ring with 600 grit SiC paper, rinsed with water, and wiped off to remove any free graphite particles. The molecular catalyst was irreversibly adsorbed on the electrode surface by means of a dip-coating procedure described previously.[17] The platinum ring was successively cleaned with a 1 μm diamond paste and a 5 μm alumina slurry and rinsed thoroughly with water after each polishing step. After sonication in water for 1 min, the ring–disk electrode was introduced into air-saturated aqueous 1 M HClO$_4$ or 1 M HCl and the platinum ring was activated by cycling between 1.20 and −0.24 V until reproducible voltammograms were obtained.

Chloride-Binding Reactions Monitored by UV–Visible Spectroscopy. The binding of chloride ions to the neutral Co(III) corrole was monitored by UV–visible spectroscopy in PhCN at room temperature (296 K). The absorbance data were then fitted to the Hill equation (eq 1).[18]

$$\log[(A_i - A_0)/(A_f - A_i)] = \log K + p \log [L] \qquad (1)$$

where A_i = absorbance at a specific concentration of ligand L, A_0 = initial absorbance where [L] = 0, and A_f = final absorbance where the fully ligated complex is the only species presented. Values of $\log K$ were obtained from the intercept of the regression line in a plot of $\log[(A_i - A_0)/(A_f - A_i)]$ versus $\log$ [py]. The slope, p, is equal to the number of axially coordinated ligands.

Chloride-Binding Reactions Monitored by Electrochemistry. The binding of chloride ions to the neutral and oxidized forms of the corroles was also monitored electrochemically by measuring the reversible half-wave potentials in CH$_2$Cl$_2$ or PhCN containing added Cl$^-$ in the form of TBACl. The relevant equations are given in the literature,[19] and the data analysis involves diagnostic plots

of $E_{1/2}$ versus log [Cl$^-$] from which both the stoichiometry and binding constants can be determined.

Chemicals and Reagents. Absolute dichloromethane (CH$_2$Cl$_2$) was obtained from Fluka Chemical Co. and used as received. Pyridine (py) was distilled over KOH under argon prior to use. Benzonitrile (PhCN) was purchased from Aldrich Chemical Co. and distilled over P$_2$O$_5$ under a vacuum prior to use. Tetra-n-butylammonium perchlorate (TBAP, Fluka Chemical Co.) was twice recrystallized from absolute ethanol and dried in a vacuum oven at 40 °C for 1 week prior to use. Tetrabutylammonium chloride (TBACl) was purchased from Sigma-Aldrich and used as received. Perchloric acid (HClO$_4$, 70%) was purchased from Mallinckrodt, while hydrochloric acid (HCl, 36.5−38.0%) was purchased from EMD and used as received.

Starting Compounds. The following examined compounds were synthesized according to previously described procedures:[10] 1-(13,17-diethyl-2,3,7,8,12,18-hexamethylporphyrin-5-yl)-8-[cobalt(III)-2,3,17,18-tetraphenyl-7,8,12,13-tetramethylcorrol-10-yl]biphenylene, (PCB)H$_2$Co; 1-(13,17-diethyl-2,3,7,8,12,13,18-hexamethylporphyrin-5-yl)-5-[cobalt(III)-2,3,17,18-tetraphenyl-7,8,12,13-tetramethylcorrol-10-yl]-9,9-dimethylxanthene, (PCX)H$_2$Co; 1-(13,17-diethyl-2,3,7,8,12,18-hexamethylporphyrin-5-yl)-8-[cobalt(III)-7,8,12,13-tetramethyl-2,3,17,18-tetraphenylcorrol-10-yl]anthracene, (PCA)-H$_2$Co; 13,17-diethyl-2,3,7,8,12,18-hexamethyl-5-phenylporphyrin, (Et$_2$Me$_6$PhPor)H$_2$;[4] and cobalt(III)-7,8,12,13-tetramethyl-2,3,10,17,18-pentaphenylcorrole, (Me$_4$Ph$_5$Cor)Co.[2]

Results and Discussion

Electrochemistry in Nonaqueous Media. The electrochemistry of the three dyads in CH$_2$Cl$_2$ and PhCN is similar to that of the related monocorrole and monoporphyrin under the same solution conditions. The half-wave potentials are listed in Table 1, and cyclic voltammograms of (PCX)H$_2$Co and (PCB)H$_2$Co in the two solvents are shown in Figure 1.

The occurrence of dimerization upon oxidation of cobalt monocorroles such as (Me$_4$Ph$_5$Cor)Co[2,3] and (OEC)Co[20] in CH$_2$Cl$_2$ or PhCN has been well-documented in the literature. This behavior is electrochemically characterized by a splitting of the first oxidation into two processes with equal current heights, each of which is half as high as the other redox reactions of the same compound. This is seen in the present study for both (PCX)H$_2$Co (Figure 1) and (PCA)H$_2$Co in CH$_2$Cl$_2$ or PhCN but not for (PCB)H$_2$Co in either solvent.
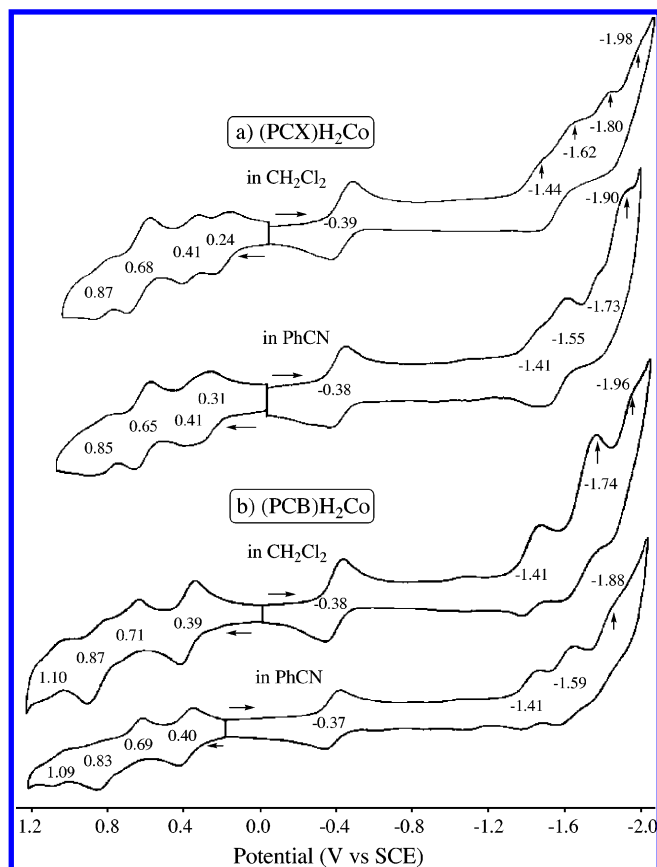
(16) Lin, X. Q.; Kadish, K. M. *Anal. Chem.* **1985**, *57*, 1489−1501.
(17) Shi, C.; Anson, F. C. *Inorg. Chem.* **1998**, *37*, 1037−1043.
(18) Ellis, J. P. E.; Linard, J. E.; Szymanski, T.; Jones, R. D.; Budge, J. R.; Basolo, F. *J. Am. Chem. Soc.* **1980**, *102*, 1889−1896.
(19) Crow, D. R. *Polarography of Metal Complexes*; Academic Press: London, 1969.
(20) Kadish, K. M.; Adamian, V. A.; Van Caemelbecke, E.; Gueletii, E.; Will, S.; Erben, C.; Vogel, E. *J. Am. Chem. Soc.* **1998**, *120*, 11986−11993.

Figure 1. Cyclic voltammograms of (a) (PCX)H$_2$Co and (b) (PCB)H$_2$Co in CH$_2$Cl$_2$ or PhCN containing 0.1 M TBAP.

The electronic interaction between equivalent redox sites has been investigated for oxidation and reduction of free-base face-to-face bisporphyrins as well as bisporphyrin derivatives containing Co(II), Zn(II), Cu(II), or Ni(II) metal ions.[21−24] The interaction between two equivalent redox sites on Co(III)[2] or Cu(III)[25] biscorroles has also been electrochemically examined for dyads with the A and B bridges linking the two macrocycles and gave separations between the two "split" $E_{1/2}$ values of 130−400 mV, depending upon the solvent and the size of the linking group.

The interaction between cobalt centers of two different (PCY)H$_2$Co dyads in solution also depends on the solvent and the linking group (Y) as shown by the cyclic voltammograms in Figure 1 and the electrochemical data in Table 1. Here, the two interacting electroactive units are proposed to be part of a $\pi-\pi$ dimer between two identical corrole units of the dyad, either (PCA)H$_2$Co or (PCX)H$_2$Co. The larger the interaction between the two cobalt corrole units of the "dimerized" (PCY)H$_2$Co, the larger will be the separation between the first two oxidation processes. The

absolute potential difference in $E_{1/2}$ between the two split oxidations of (PCX)H$_2$Co (Figure 1a; $\Delta E_{1/2}$) is equal to 170 mV in CH$_2$Cl$_2$ and 100 mV in PhCN, while $\Delta E_{1/2}$ for (PCA)H$_2$Co is 150 mV in CH$_2$Cl$_2$ and 100 mV in PhCN (see Table 1). The separations in half-wave potentials for (PCA)H$_2$Co and (PCX)H$_2$Co in CH$_2$Cl$_2$ can be compared to a $\Delta E_{1/2}$ of 170 mV for the monocorrole, (Me$_4$Ph$_5$Cor)Co, under the same solution conditions,[2,3] but no dimerization occurs for the monocorrole in PhCN.[3] The fact that no dimerization is observed for (PCB)H$_2$Co in PhCN or CH$_2$Cl$_2$ (that is, no splitting of the first oxidation) can be attributed to a stronger internal $\pi-\pi$ interaction between the two macrocycles of the dyad, which would tend to weaken any $\pi-\pi$ interaction between the corrole macrocycles of two separate (PCB)H$_2$Co complexes.

Further differences between current-voltage curves of the three dyads in CH$_2$Cl$_2$ or PhCN involve the Co(III)/Co(II) process. This reaction occurs at $E_{1/2} = -0.37$ to -0.39 V for (PCX)H$_2$Co or (PCB)H$_2$Co (see Table 1), while the same metal-centered electrode reaction of (PCA)H$_2$Co is located at $E_{1/2} = -0.20$ V in CH$_2$Cl$_2$ and -0.26 V in PhCN. The half-wave potentials for the Co(III)/Co(II) reactions of the three dyads are all more negative than $E_{1/2}$ values for reduction of the monocorrole (-0.15 to -0.16 V) in the same nonaqueous solvents (Table 1). This parallels what has been observed for other related biscorroles and porphyrin−corrole dyads having B or A bridges[1a,4,5] and can be accounted for by an increased interaction between the two face-to-face π systems of the dyads, which are close to each other and, thus, have a more negative reduction potential. The larger the internal interaction between the two π systems of the dyad, the harder the reduction, and this leads to the following proposed order of internal $\pi-\pi$ interaction between the porphyrin and corrole macrocycles in the currently investigated series of compounds: (PCA)H$_2$Co < (PCX)H$_2$Co $\approx$ (PCB)H$_2$Co.

UV−Visible Spectra of Initial Compounds. UV−visible spectral data for the three dyads in PhCN and CH$_2$Cl$_2$ are shown in Table 2. The Soret band of the 9,9-dimethylxanthene (X)- and biphenylene (B)-bridged compounds are at similar wavelengths and blue-shifted by 10−13 nm as compared to λ_{max} of the anthracene (A)-bridged compound in the same two solvents. In addition, all three dyads show an additional weak band at 623−630 nm, which is also seen for (Et$_2$Me$_6$PhPor)H$_2$ but not for (Me$_4$Ph$_5$Cor)Co, thus, providing evidence that this latter band is associated with the free-base porphyrin macrocycle of the dyad. The Soret region of the spectrum is also dominated by porphyrin transitions in the case of the dyads, and this is most evident in Table 2 by the similarity in λ_{max} and ϵ values for bands in the spectra of the three dyads and the monoporphyrin, (Et$_2$Me$_6$PhPor)H$_2$.

Chloride Binding to the Cobalt Center of the Monocorrole. To investigate the effect of Cl$^-$ on the electrode reactions of (PCY)H$_2$Co, we first characterized the electrochemistry of the monocorrole, (Me$_4$Ph$_5$Cor)Co, in PhCN containing 0.1 M TBAP and excess Cl$^-$. These results are discussed below and provide clear evidence for the binding

(21) Le Mest, Y.; L'Her, M.; Hendricks, N. H.; Kim, K.; Collman, J. P. *Inorg. Chem.* **1992**, *31*, 835−847.
(22) Le Mest, Y.; L'Her, M.; Saillard, J.-Y. *Inorg. Chim. Acta* **1996**, *248*, 181−191.
(23) Le Mest, Y.; L'Her, M.; Courtot-Coupez, J.; Collman, J. P.; Evitt, E. R.; Bencosme, C. S. *J. Electroanal. Chem.* **1985**, *184*, 331−346.
(24) Le Mest, Y.; L'Her, M.; Collman, J. P.; Kim, K.; Hendricks, N. H.; Helm, S. *J. Electroanal. Chem.* **1987**, *234*, 277−295.
(25) Guilard, R.; Gros, C. P.; Barbe, J.-M.; Espinosa, E.; Jérôme, F.; Tabard, A.; Latour, J.-M.; Shao, J.; Ou, Z.; Kadish, K. M. *Inorg. Chem.* **2004**, *43*, 7441−7455.

Table 2. UV−Visible Spectral Data (λ_{max}, $\epsilon \times 10^{-4}$ L mol^{-1} cm^{-1}) for (PCY)H$_2$Co Dyads in Different Solvents

solvent	compound	Soret region		visible region[a]			
PhCN	(Me$_4$Ph$_5$Cor)Co	399 (8.9)	535 (2.3)				
	(Et$_2$Me$_6$PhPor)H$_2$	407 (19.4)	503 (1.8)	535 (0.9)	572 (0.9)	625 (0.4)	
	(PCA)H$_2$Co	405 (15.2)	507 (2.4)	538 (1.9)	574 (1.5)	627 (0.8)	
	(PCX)H$_2$Co	394 (21.8)	507 (2.4)	538 (1.9)	572 (1.5)	625 (0.7)	
	(PCB)H$_2$Co	392 (14.3)	507 (1.7)	530 (1.6)^{sh}	575 (1.0)^{sh}	626 (0.5)^{sh}	
CH$_2$Cl$_2$	(Me$_4$Ph$_5$Cor)Co	398 (4.5)	529 (1.1)				
	(Et$_2$Me$_6$PhPor)H$_2$	402 (15.7)	501 (1.3)	534 (0.7)	571 (0.6)	623 (0.3)	
	(PCA)H$_2$Co	397 (14.7)	507 (2.2)	535 (1.9)	570 (1.1)^{sh}	627 (0.5)	
	(PCX)H$_2$Co	387 (16.6)	507 (2.1)	536 (1.8)	571 (1.0)^{sh}	630 (0.4)	
	(PCB)H$_2$Co	387 (15.8)	505 (1.8)	528 (1.6)^{sh}	573 (1.0)^{sh}	629 (0.4)^{sh}	

[a] sh = shoulder.

of Cl$^-$ to the electrogenerated Co(IV) form of the mono-corrole as well as to the initial Co(III) species under conditions of higher chloride concentration.

Figure 2 illustrates cyclic voltammograms of the cobalt corrole monomer, (Me$_4$Ph$_5$Cor)Co, in PhCN and 0.1 M TBAP containing different concentrations of added TBACl. The examined potential range was from −0.8 to 1.4 V in PhCN containing 0.1 M TBAP, but the anodic (positive) limit was not extended beyond +0.60 V in solutions of TBACl in order to avoid the oxidation of Cl$^-$ that occurs at about 0.8 V. Three well-defined processes are seen under all solution conditions, with the most positive $E_{1/2}$ values being observed in PhCN and 0.1 M TBAP and the most negative

in PhCN containing the highest concentrations of added TBACl.

The data in Figure 2 are consistent with the binding of Cl$^-$ to (Me$_4$Ph$_5$Cor)Co^{III}, [(Me$_4$Ph$_5$Cor)Co^{IV}]$^+$, and [(Me$_4$Ph$_5$Cor$^{•+}$)Co^{IV}]$^{2+}$, which results in a shift of $E_{1/2}$ values for all three processes toward more negative potentials. The magnitude of the shift between solutions containing 0.1 M TBAP and those with 0.1 M TBAP plus 60 equiv of Cl$^-$ amounts to 80 mV in the case of the Co(III)/Co(II) reaction (−0.16 → −0.24 V), 410 mV in the case of the Co(IV)/Co(III) reaction (0.47 → 0.06 V), and 450 mV in the case of the Co(IV) radical/Co(IV) process (0.72 → 0.27 V).

A linear relationship is obtained between half-wave potentials for the first oxidation of (Me$_4$Ph$_5$Cor)Co to its Co(IV) form and log [TBACl] in PhCN (the middle process in Figure 2), and the slope of −56 mV (Figure 3a) is close to the predicted theoretical Nernstian value of −59 mV for an electrode reaction involving the loss of one axially bound Cl$^-$ ligand upon conversion of Co(IV) to Co(III).

The Co(IV) center of [(Me$_4$Ph$_5$Cor)Co^{IV}]$^+$ can axially bind one or two Cl$^-$ ligands, and thus, either of the two electrode reactions given by eqs 2 and 3 could account for the −56 mV slope in Figure 3a.

$$(Me_4Ph_5Cor)Co^{IV}Cl + e^- \rightleftharpoons (Me_4Ph_5Cor)Co^{III} + Cl^- \quad (2)$$

$$[(Me_4Ph_5Cor)Co^{IV}Cl_2]^- + e^- \rightleftharpoons$$
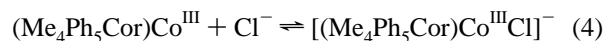$$[(Me_4Ph_5Cor)Co^{III}Cl]^- + Cl^- \quad (3)$$
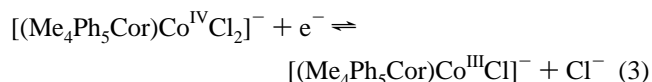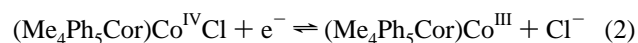
On the basis of results for the related (PCY)MClCoCl complexes [M = Fe(III) or Mn(III)],[7] the electrochemical reduction shown by eq 2 most likely occurs in PhCN solutions containing 1 equiv of Cl$^-$, but at higher concentrations of chloride, the prevailing reaction in PhCN involves reduction of a bis-Cl Co(IV) complex to a mono-Cl Co(III) species, as shown in eq 3. Electrochemistry alone cannot differentiate the above two possibilities in solutions containing greater than 2 equiv of Cl$^-$, but the prevailing electron transfer mechanism can easily be determined by independently measuring the binding of Cl$^-$ to the Co(III) form of the monocorrole using UV−visible spectroscopy. These results are shown in Figure 3b, which illustrates the changes observed during a spectrally monitored titration of (Me$_4$Ph$_5$Cor)Co in PhCN with increasing amounts of TBACl. The spectral changes at 534 and 566 nm were analyzed by
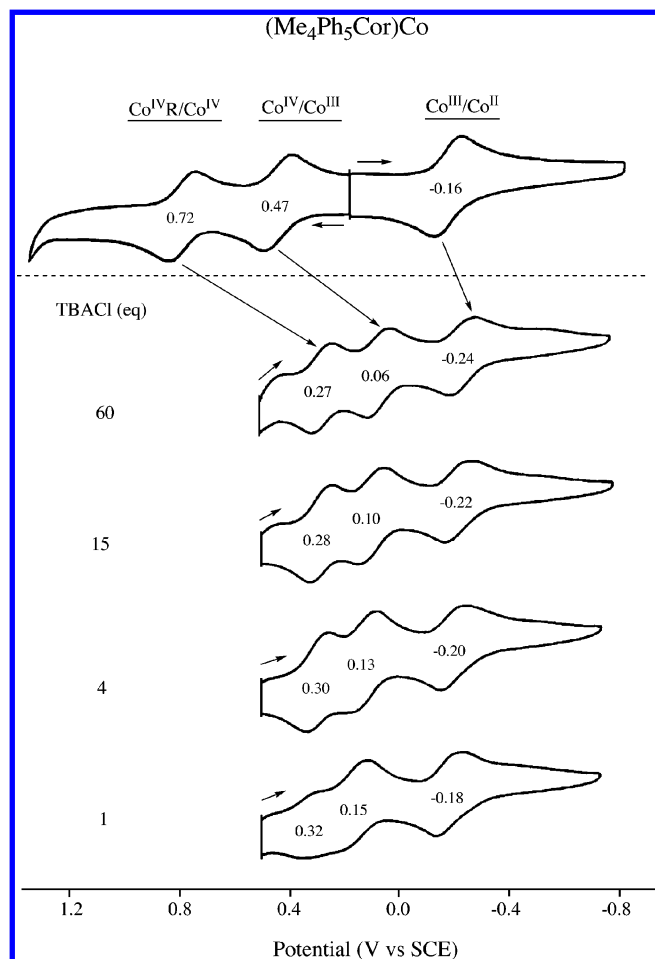
**Figure 2.** Cyclic voltammograms of (Me$_4$Ph$_5$Cor)Co in PhCN containing 0.1 M TBAP and 0−60 equiv of TBACl.
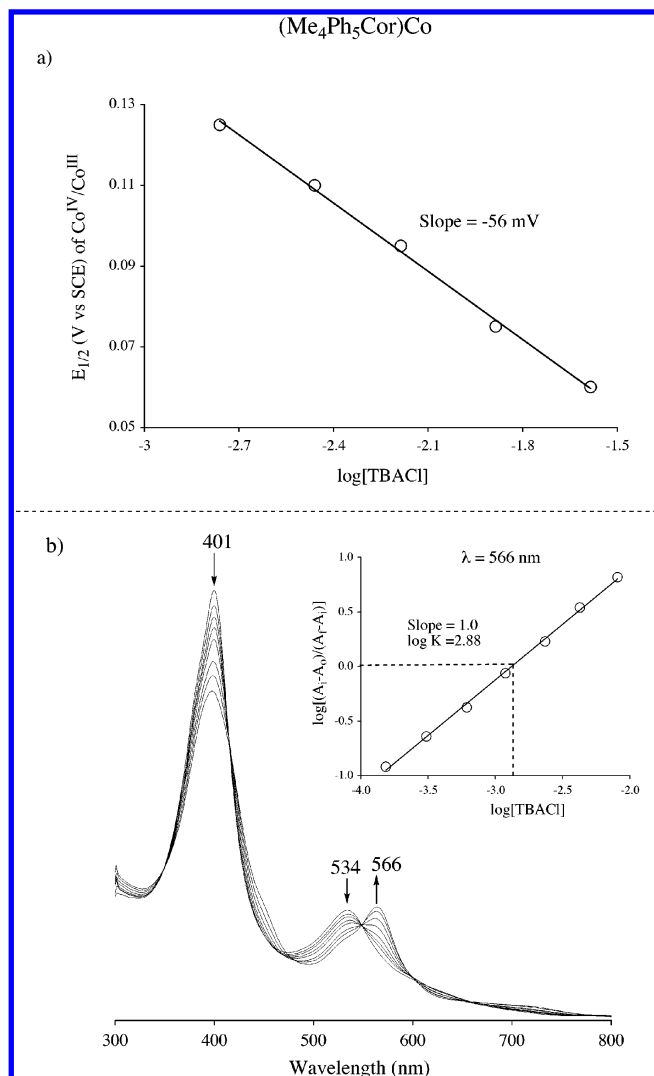
Figure 3. (a) Plot of $E_{1/2}$ for the $[Co^{IV}Cl_2]^-/[Co^{III}Cl]^-$ process of $(Me_4Ph_5Cor)Co$ in PhCN and 0.1 M TBAP vs log [TBACl] added to solution and (b) UV−visible spectral changes of 2.5×10^{-5} M $(Me_4Ph_5Cor)Co$ in PhCN with increasing TBACl concentrations from 1.5×10^{-4} to 8.1×10^{-3} M. Inset shows the Hill plot.

plotting $\log[(A_i - A_o)/(A_f - A_i)]$ versus log [TBACl], and the latter correlation is shown in the inset of Figure 3b where the slope of the line is 1.0, thus demonstrating that only one Cl^- ligand is bound to $(Me_4Ph_5Cor)Co^{III}$ with a log $K =$ 2.88. The prevailing axial ligand binding reaction to Co(III) is given by eq 4 and, when combined with the electrochemical data in Figure 3a, eliminates the reaction in eq 2 as a possible electron transfer mechanism in PhCN solutions containing high Cl^- concentrations.

$$(Me_4Ph_5Cor)Co^{III} + Cl^- \rightleftharpoons [(Me_4Ph_5Cor)Co^{III}Cl]^- \quad (4)$$

It is interesting to note that the UV−visible spectrum for $[(Me_4Ph_5Cor)Co^{III}Cl]^-$ in PhCN is virtually identical in its Q-band region to the spectrum of the mono-CO adduct, $(Me_4Ph_5Cor)Co(CO)$, which has a band at 567 nm and a shoulder at 548 nm in CH_2Cl_2.[2] This similarity is shown in Figure S1 (Supporting Information) where the major Q band of $[(Me_4Ph_5Cor)CoCl]^-$ is at 566 nm and a shoulder is at 546 nm.

In summary, the addition of one Cl^- ligand to $(Me_4Ph_5Cor)Co^{III}$ generates $[(Me_4Ph_5Cor)Co^{III}Cl]^-$, which is electrochemically oxidized to $[(Me_4Ph_5Cor)Co^{IV}Cl_2]^-$ in the presence of excess Cl^- according to the electrode reaction given by eq 3. A knowledge of this stoichiometry, when combined with the log $K = 2.88$ for reaction 4, the Nernstian slope of the line in Figure 3a, and the classical Lingane equation[19] then enables a calculation of the binding constant for the addition of two Cl^- ligands to $[(Cor)Co^{IV}]^+$. This ligand addition reaction is shown in eq 5, where log $\beta_2 =$ 11.4.

$$[(Me_4Ph_5Cor)Co^{IV}]^+ + 2Cl^- \rightleftharpoons [(Me_4Ph_5Cor)Co^{IV}Cl_2]^- \quad (5)$$
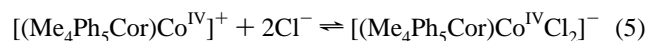
In the same manner, the 450 mV negative shift in $E_{1/2}$ (from 0.72 to 0.27 V) for the second oxidation in PhCN, 0.1 M TBAP upon the addition of ≥ 60 equiv of Cl^- enables calculation of the Cl^- binding constant for the doubly oxidized complex, $[(Me_4Ph_5Cor^{\bullet+})Co^{IV}]^{2+}$, which is a Co(IV) corrole π-cation radical. This reaction is shown in eq 6, where log $\beta_2 = 19.0$.

$$[(Me_4Ph_5Cor^{\bullet+})Co^{IV}]^{2+} + 2Cl^- \rightleftharpoons (Me_4Ph_5Cor)Co^{IV}Cl_2 \quad (6)$$
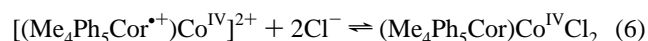
The above calculation was done by inserting the value of log $\beta_2 = 11.4$ for Cl^- binding to Co(IV) (eq 5) into eq 7, where $\beta_{2,Co(IV)}$ describes Cl^- binding as seen in eq 5 and $\beta_{2,Co(IV) \text{ radical}}$ the Cl^- binding shown in eq 6.[19] A similar method has been used in the past for elucidating pyridine binding constants to a number of oxidized porphyrins, one of which is (TPP)Zn.[26,27]

$$\Delta E_{1/2} = \frac{0.059}{n} \log \frac{\beta_{2,Co(IV)\text{radical}}}{\beta_{2,Co(IV)}} \quad (7)$$

The Co(II) corrole in electrogenerated $[(Me_4Ph_5Cor)Co]^-$ does not bind Cl^-, as clearly seen by a comparison of the UV−visible spectrum for the singly reduced complex in PhCN with and without added Cl^- (Figure 4b and d). The anionic Co(II) corrole in PhCN and 0.1 M TBAP exhibits a spectrum with the Soret band at 424 nm and two visible bands at 561 and 642 nm (Figure 4d). The same spectrum is obtained in PhCN containing 0.1 M TBAP plus 100 equiv of added Cl^- (Figure 4b).

The UV−visible spectral changes obtained during the first oxidation of $(Me_4Ph_5Cor)Co$ [the Co(III)/Co(IV) process] with and without added Cl^- are also shown in Figure 4a and c. The spectra of the singly oxidized species are different from each other under the different solution conditions. $[(Cor)Co^{IV}(Cl)_2]^-$, generated in a PhCN solution containing 0.1 M TBAP and 100 equiv of TBACl (Figure 4a) has a broad Soret band with a maximum at 448 nm and a weak visible band located at 731 nm. In contrast, the $[(Cor)Co^{IV}]^+$ species generated in PhCN solutions with no added TBACl (Figure 4c) has a split Soret band at 383 and 442 nm and a weak visible band at 680 nm.
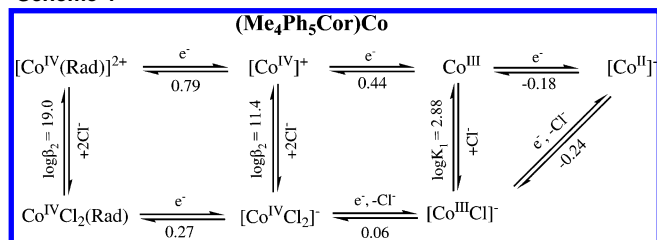
(26) Kadish, K. M.; Shiue, L. R.; Rhodes, R. K.; Bottomley, L. A. *Inorg. Chem.* **1981**, *20*, 1274−1277.
(27) Kadish, K. M.; Rhodes, R. K. *Inorg. Chem.* **1981**, *20*, 2961−296.
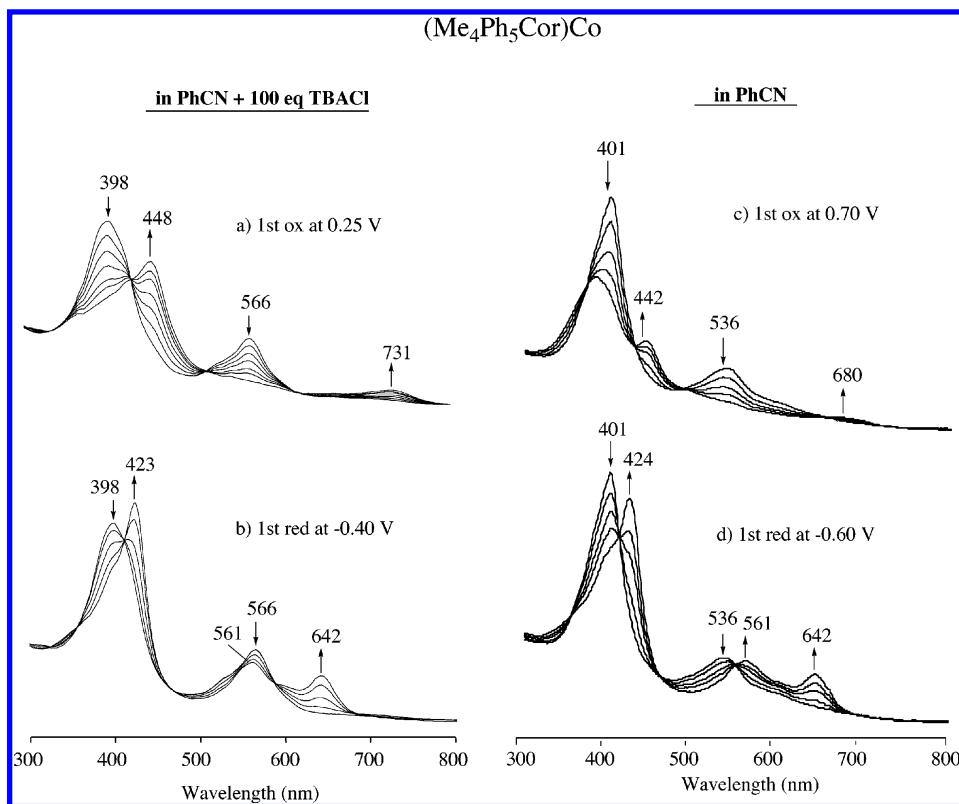
Figure 4. UV-visible spectral changes for (a) oxidation and (b) reduction of (Me$_4$Ph$_5$Cor)Co in PhCN and 0.1 M TBAP containing 100 equiv of TBACl as compared to (c) oxidation and (d) reduction of the same solution not containing TBACl.

Scheme 1

The spectral and electrochemical data for the three investigated cobalt corrole redox processes of the monocorrole, namely, Co^{IV} radical/Co^{IV}, Co^{IV}/Co^{III}, and Co^{III}/Co^{II}, are self-consistent in the presence and absence of added Cl$^-$, and the overall electron transfer and Cl$^-$ addition processes are presented in Scheme 1, where the upper pathway describes the redox reactions in PhCN, 0.1 M TBAP and the lower one the reactions in the same solutions containing 60 equiv of added TBACl. The chloride binding constants for each oxidation state of the monocorrole are shown in Scheme 1 and range from log β_2 = 19.0 for the Co^{IV} corrole π-cation radical to log K_1 = 2.88 for the neutral Co^{III} form of the compound.

Chloride Binding to (PCY)H$_2$Co. Binding of Cl$^-$ to the cobalt center of the three dyads in their various oxidation states was also electrochemically investigated in PhCN containing 0.1 M TBAP and Cl$^-$ added stepwise in the form of TBACl. Examples of the resulting cyclic voltammograms are shown in Figure 5a for (PCA)H$_2$Co in PhCN containing 0−160 equiv of added TBACl, and a plot of $E_{1/2}$ for the Co(IV)/Co(III) process versus log [TBACl] is shown in Figure 5b. The initial voltammogram in PhCN and 0.1 M

TBAP is characterized by a Co(III)/Co(II) reduction at $E_{1/2}$ = −0.26 V and two oxidations, the first of which is split into two overlapping processes indicative of weak dimerization of the two dyads as compared to what is observed in the case of (PCX)H$_2$Co (see Figure 1).

The cyclic voltammograms of (PCA)H$_2$Co in PhCN containing TBACl are similar to what is observed for the monocorrole, (Me$_4$Ph$_5$Cor)Co, under similar solution conditions (see Figure 2). The stepwise abstraction of two electrons from the corrole unit of (PCA)H$_2$Co occurs at $E_{1/2}$ values that, in the presence of added Cl$^-$, are substantially shifted toward negative potentials as compared to the oxidations in PhCN and 0.1 M TBAP, consistent with a strong binding of Cl$^-$ to the singly and doubly oxidized forms of the dyad. No shift in $E_{1/2}$ is observed for the Co(III)/Co(II) process of (PCA)H$_2$Co upon Cl$^-$ addition nor are any UV−visible spectral changes observed for neutral (PCA)H$_2$Co upon addition of Cl$^-$, thus indicating the lack of Cl$^-$ binding to the Co(III) or electrogenerated Co(II) centers of the PCA complex.

The number of Cl$^-$ ligands bound to the Co(IV) unit of singly oxidized (PCA)H$_2$Co was obtained by analyzing the potential shift of the Co(IV)/Co(III) process as a function of increasing Cl$^-$ concentration, and the relevant diagnostic plot is shown in Figure 5b. A straight line slope of −57 mV is obtained, consistent with the predicted theoretical slope of −59 mV for a reaction involving the loss of one Cl$^-$ ligand upon going from the singly oxidized Co(IV) corrole to its neutral Co(III) form. Combining this result with the fact that the Co(III) in (PCA)H$_2$Co does not bind Cl$^-$ (see above
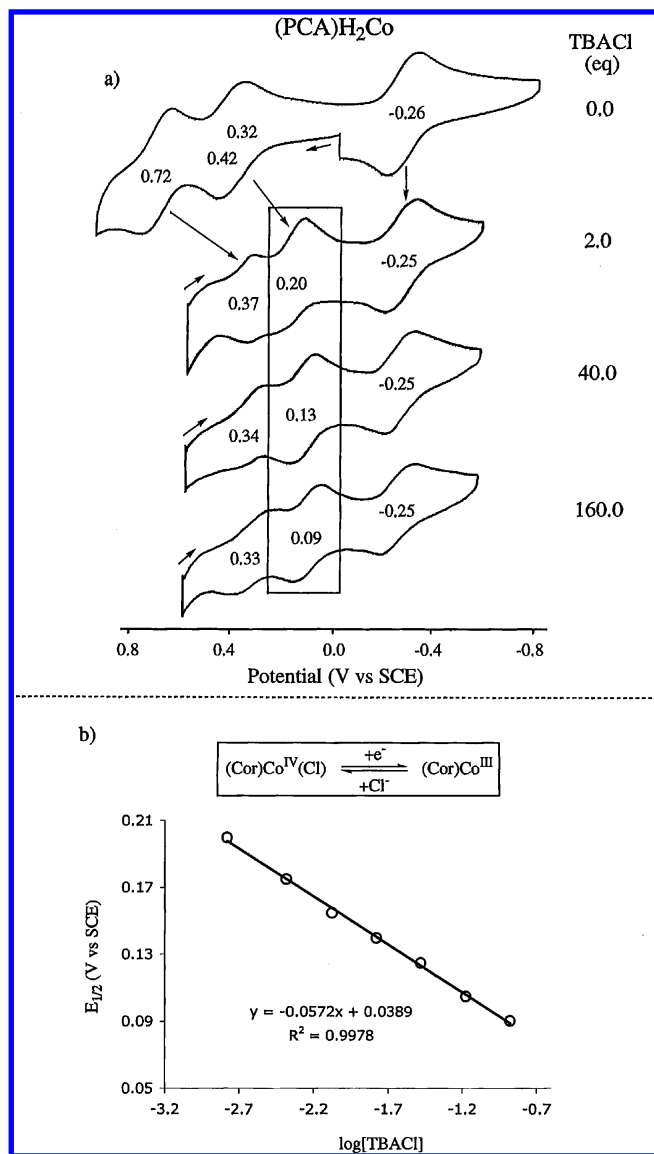
Figure 5. (a) Cyclic voltammograms of (PCA)H$_2$Co in PhCN and 0.1 M TBAP with added TBACl and (b) plot of $E_{1/2}$ for the Co^{IV}Cl/Co^{III} process vs log [TBACl].

discussion) leads to the conclusion that the Co(IV) corrole in [(PCA)H$_2$Co^{IV}]$^+$ binds only one Cl$^-$ axial ligand to give (PCA)H$_2$Co^{IV}Cl in solutions containing added Cl$^-$.

The formation constant for the binding of one Cl$^-$ ligand to [(PCA)H$_2$Co^{IV}]$^+$ was calculated using the Lingane equation[19] combined with the data in Figure 5b and gives a log $K_1 = 6.5$ for the reaction shown in eq 8.

$$[(PCA)H_2Co^{IV}]^+ + Cl^- \rightleftharpoons (PCA)H_2Co^{IV}Cl \quad (8)$$
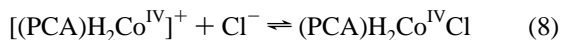
The Cl$^-$ axial ligand dissociates during the Co(IV) $\rightleftharpoons$ Co(III) reaction, and the relevant redox process is then given by eq 9.

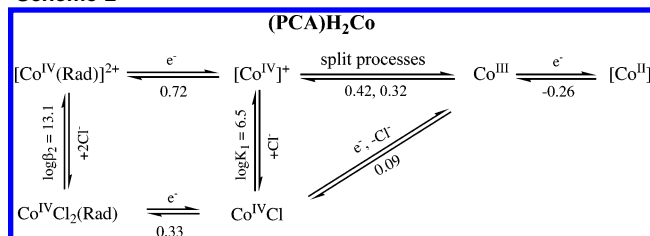$$(PCA)H_2Co^{IV}Cl + e^- \rightleftharpoons (PCA)H_2Co^{III} + Cl^- \quad (9)$$
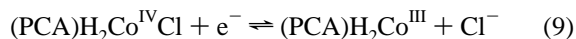
The $E_{1/2}$ for the above reaction is 0.20 V in PhCN solutions containing 2 equiv of Cl$^-$ and shifts to 0.09 V in solutions containing 160 equiv of Cl$^-$ (Figure 5a). Both half-wave potentials are within the range of $E_{1/2}$ values for the Co^{IV}Cl

Table 3. Half-Wave Potentials (V vs SCE) of (PCY)H$_2$Co in PhCN and 0.1 M TBAP

	PhCN			PhCN + excess Cl$^-$ (160 equiv)		
compound	second ox	first ox	first red	second ox	first ox	first red
(PCA)H$_2$Co	0.72	0.42, 0.32	−0.26	0.33	0.09	−0.25
(PCX)H$_2$Co	0.65	0.41, 0.31	−0.38	a	0.05	−0.38
(PCB)H$_2$Co	0.69	0.40	−0.37	a	0.07	−0.37
(Me$_4$Ph$_5$Cor)Co	0.72	0.47	−0.16	0.27^b	0.06^b	−0.25^b

^{a} Reaction occurs at $E_{1/2}$ values beyond the positive potential limit of the solvent with 160 equiv of Cl$^-$ ($\sim$0.60 V vs SCE). ^{b} PhCN + 120 equiv of Cl$^-$.

Scheme 2

$\rightleftharpoons$ Co^{III} process of the same corrole linked in a face-to-face orientation to Fe^{III} or Mn^{III} porphyrins.[7]

A further oxidation of (PCA)H$_2$Co^{IV}Cl to its Co(IV) π-cation radical form in PhCN solutions containing 160 equiv of Cl$^-$ gives (PCA)H$_2$Co^{IV}Cl$_2$ at $E_{1/2} = 0.33$ V, and this half-wave potential, which remains invariant with further additions of Cl$^-$ to solution, can be compared to the measured $E_{1/2} = 0.27$ V for the same redox process of monomeric (Me$_4$-Ph$_5$Cor)Co under similar solution conditions (see Figure 2 and Table 3). The $E_{1/2} = 0.33$ V for the above process can also be combined with the $E_{1/2} = 0.72$ V for the same electrode reaction in the absence of TBACl (see Figure 5a), and using eq 7 leads to a log $\beta_2 = 13.1$ for the binding of 2Cl$^-$ to the doubly oxidized Co(IV) π-cation radical.

The proposed mechanism for the oxidation and reduction of the cobalt center in (PCA)H$_2$Co is given in Scheme 2 and differs from the monocorrole in two aspects. The first is that Cl$^-$ does not coordinate to Co(III) in the dyad, and the second is that only one Cl$^-$ ligand binds to Co(IV) in PhCN solutions containing up to 160 equiv of TBACl.

Electrochemically monitored chloride titrations were also carried out for (PCX)H$_2$Co (Figure 6) and (PCB)H$_2$Co (Figure S2, Supporting Information). The (PCX)H$_2$Co complex in CH$_2$Cl$_2$ or PhCN containing 0.1 M TBAP has a first oxidation that is split into two processes of equal current height, indicating a π−π dimerization between corrole macrocycles of two different (PCX)H$_2$Co species. The dimer is broken up upon addition of 1.0 equiv of Cl$^-$ to the solution (see Figure 6c), and under these conditions, the two reversible oxidations in Figure 6a are replaced by an irreversible Co(IV)/Co(III) process with a coupled reduction at $E_{pc} = 0.03$ V and an oxidation at $E_{pa} = 0.28$ V for a scan rate of 0.1 V/s. The split peaks then merge into a single reversible oxidation/reduction couple at higher Cl$^-$ concentrations, and this is shown by the cyclic voltammogram in Figure 6d. The second oxidation of the corrole unit is not seen under these conditions.
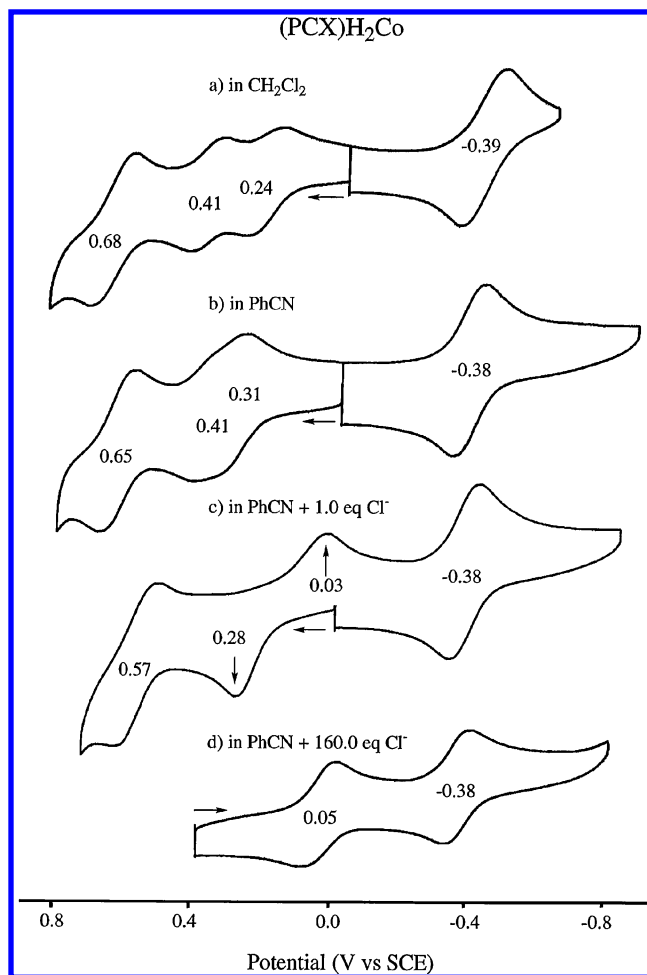
Figure 6. Cyclic voltammograms of (PCX)H$_2$Co in the following solutions containing 0.1 M TBAP: (a) CH$_2$Cl$_2$, (b) PhCN, (c) PhCN + 1 equiv of TBACl, and (d) PhCN + 160 equiv of TBACl.

A dimerization between the two oxidized dyads does not occur for (PCB)H$_2$Co in CH$_2$Cl$_2$ or PhCN. Here, a reversible one-electron oxidation is seen at $E_{1/2}$ = 0.40 V in PhCN and 0.1 M TBAP (Figure S2, Supporting Information), but the Co(IV)/Co(III) reaction becomes irreversible in PhCN solutions containing 1.2−40 equiv of added Cl$^-$. Like (PCX)H$_2$Co, this electrode reaction is reversible in PhCN solutions containing 160 equiv of TBACl, but no second oxidation of the corrole unit could be seen up to the anodic potential limit of the solvent where the added excess Cl$^-$ is oxidized (∼0.6 V vs SCE).

The half-wave potentials for the Co(III)/Co(II) reductions of (PCX)H$_2$Co, (PCB)H$_2$Co, and (PCA)H$_2$Co in PhCN occur at $E_{1/2}$ values that are invariant with the addition of Cl$^-$ (see Figures 5, 6, and S2), indicating that neither Co(III) nor Co(II) axially binds Cl$^-$ in solutions of PhCN. Half-wave potentials for the oxidation and reduction of the three dyads in PhCN containing 0.1 M TBAP and 160 equiv Cl$^-$ are summarized in Table 3, which also includes data on (Me$_4$Ph$_5$Cor)Co.

Attempts were made to calculate Cl$^-$ binding constants by the Co(IV) ion of the PCX and PCB derivatives, but plots of $E_{1/2}$ versus log [TBACl] gave non-Nernstian slopes due to slow kinetics, and therefore, no reliable thermodynamic data could be obtained.

Redox Properties of (PCA)H$_2$Co, (PCB)H$_2$Co, and (PCX)H$_2$Co and the Catalytic Reduction of O$_2$ in 1 M HClO$_4$. The catalytic activity of the (PCY)H$_2$Co dyads toward the reduction of O$_2$ was examined by cyclic voltammetry and rotating ring-disk electrode voltammetry in aqueous solutions of 1 M HClO$_4$. Current−potential curves recorded at a graphite disk coated with (PCA)H$_2$Co and (PCB)H$_2$Co are illustrated in Figure 7. In the absence of dioxygen, the response of the graphite electrode coated with (PCA)H$_2$Co resembles that obtained with the (PCB)H$_2$Co-coated electrode (Figure 7a). The cyclic voltammogram of (PCB)H$_2$Co shows two reversible processes located at $E_{1/2}$ = 0.37 and −0.02 V in 1 M HClO$_4$, whereas the (PCA)H$_2$Co system is characterized by a reversible process at $E_{1/2}$ = 0.36 V and an irreversible reduction peak at E_{pc} = −0.12 V. On the basis of comparisons with the electrochemical response of (Me$_4$Ph$_5$Cor)Co adsorbed on a graphite electrode ($E_{1/2}$ = 0.38, 0.20, and −0.08 V),[8] the two processes of (PCB)H$_2$Co at $E_{1/2}$ = 0.37 and −0.02 V can be assigned to the formal potentials of the Co(IV)/Co(III) and Co(III)/Co(II) couples, respectively. The presence of an additional reversible process at $E_{1/2}$ = 0.20 V for (Me$_4$Ph$_5$Cor)Co was earlier explained by the tendency of the corrole to spontaneously dimerize[8] (or to form higher aggregates) on the graphite surface. This electrochemical behavior is not observed for the three investigated free-base porphyrin−cobalt corrole dyads.

When the solution is saturated with air (Figure 7b), the response of the (PCY)H$_2$Co-coated electrodes is characterized by a large reduction peak located at E_{pc} = 0.29−0.31 V, depending upon the spacer (see exact values in Table 4). The electroreduction of O$_2$ by the three (PCY)H$_2$Co dyads occurs at slightly less positive potentials than that of the related cobalt(III) corrole, (Me$_4$Ph$_5$Cor)Co (E_{pc} = 0.36 V),[8] but leaves no doubt that the electrocatalysis proceeds at the potential of the Co(IV)/Co(III) process, with the cobalt(III) center of the dyad being the active site in the electroreduction of O$_2$.

The rotating ring-disk electrode responses obtained for (PCA)H$_2$Co and (PCB)H$_2$Co adsorbed on the graphite electrode in 1 M HClO$_4$ (Figure 7c) exhibit a single wave for the reduction of O$_2$ ($E_{1/2}$ = 0.35 V) as does (PCX)H$_2$Co, and the average number of electrons transferred (n) is higher than 2 (Table 4) for all three investigated porphyrin−corrole dyads. The number of electrons transferred in the O$_2$ electroreduction process ranges from 2.5 to 2.9 for (PCY)H$_2$Co and (Me$_4$Ph$_5$Cor)Co,[8] indicating that the electrocatalytic reduction of O$_2$ leads to formation of H$_2$O$_2$ and H$_2$O through processes involving both 2e$^-$ and 4e$^-$ reactions, as was previously reported for monocobalt cofacial bisporphyrins.[12] This is clearly different from the porphyrin−corrole dyads with two cobalt centers, (PCY)Co$_2$ (Y = O, A, X, and B),[8] where n = 3.5−3.9 and O$_2$ is mainly reduced to H$_2$O through a 4e$^-$ process.

The unmetalated porphyrin unit of the (PCY)H$_2$Co dyads may increase the selectivity for the four-electron reduction of O$_2$ to H$_2$O over the two-electron pathway by helping to stabilize the partially reduced dioxygen species. A similar effect has been reported for face-to-face bisporphyrin systems
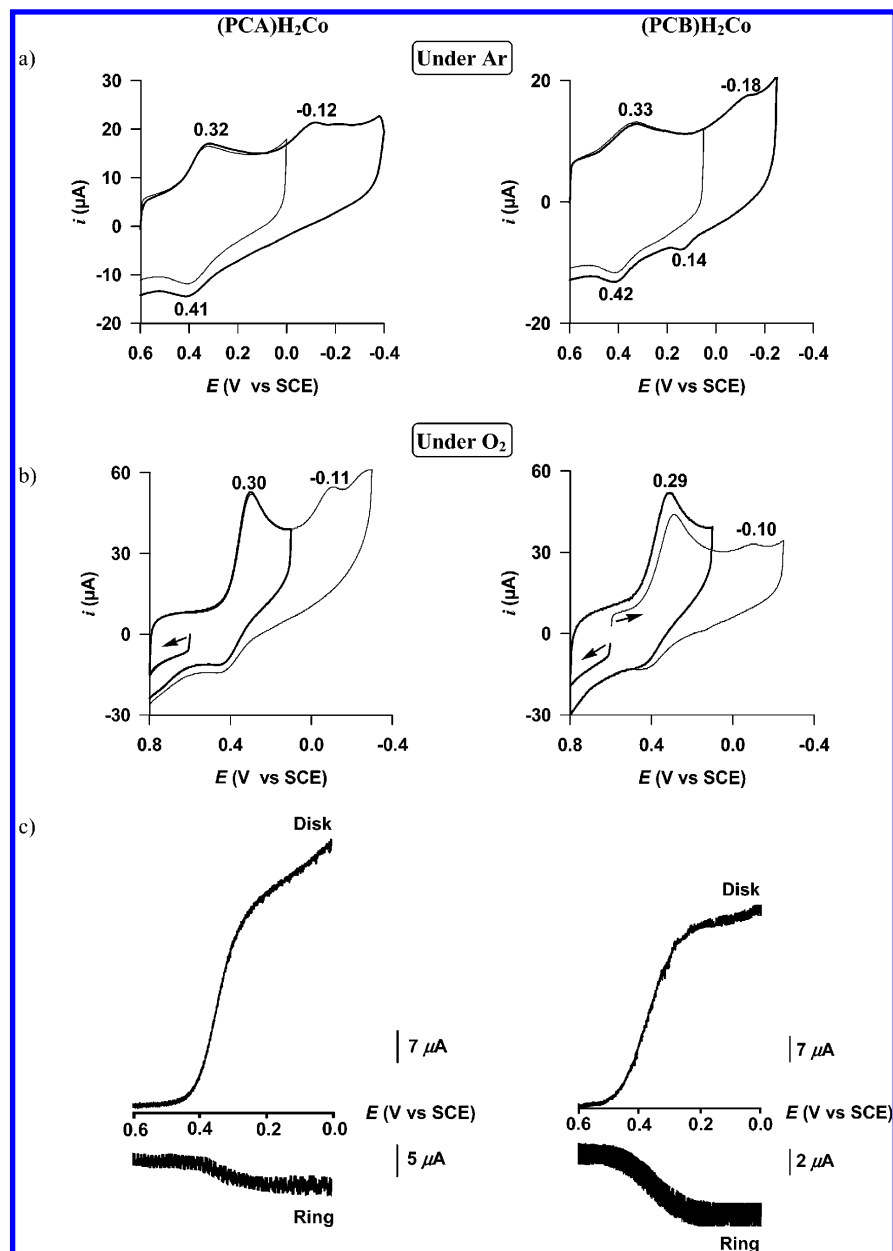
Figure 7. (a) Cyclic voltammograms of (PCA)H$_2$Co (left) and (PCB)H$_2$Co (right) adsorbed on an EPG electrode. Supporting electrolyte: 1 M HClO$_4$ saturated with argon. Scan rate: 50 mV/s. (b) Cyclic voltammograms of (PCA)H$_2$Co (left) and (PCB)H$_2$Co (right) adsorbed on an EPG electrode. Supporting electrolyte: 1 M HClO$_4$ saturated with O$_2$. [O$_2$] = 0.24 mM. Scan rate: 50 mV/s. (c) Reduction of O$_2$ at a rotating ring (pt)-disk (EPG) electrode coated with (PCA)H$_2$Co (left) and (PCB)H$_2$Co (right) in air-saturated 1 M HClO$_4$. The potential of the ring electrode was maintained at 1.1 V. Rotating rate: 100 rpm. Scan rate: 5 mV/s.

containing one free-base porphyrin and one cobalt porphyrin.[28] Alternatively, the increased value of *n* above 2.0 may be due to the presence of aggregates or dimers of the dyads on the electrode surface, as was postulated to occur in the case of (Me$_4$Ph$_5$Cor)Co(III),[8] (OEP)Co(II),[29] and Co(II) porphine.[30] A dimerization is not detected by electrochemistry of the dyads in HCl or HClO$_4$, but it is clearly evident from the cyclic voltammograms of (PCX)H$_2$Co and (PCA)H$_2$Co in CH$_2$Cl$_2$ or PhCN (see Figures 1 and 6 and Table 4).

(28) Ni, C.-L.; Abdalmuhdi, I.; Chang, C. K.; Anson, F. C. *J. Phys. Chem.* **1987**, *91*, 1158−1166.
(29) Song, E.; Shi, C.; Anson, F. C. *Langmuir* **1998**, *14*, 4315−4321.
(30) Shi, C.; Steiger, B.; Yuasa, M.; Anson, F. C. *Inorg. Chem.* **1997**, *36*, 4294−4295.

Table 4. Electroreduction of Dioxygen by Adsorbed Free-Base Porphyrin−Cobalt Corrole Dyads in Air-Saturated 1 M HClO$_4$ or 1 M HCl
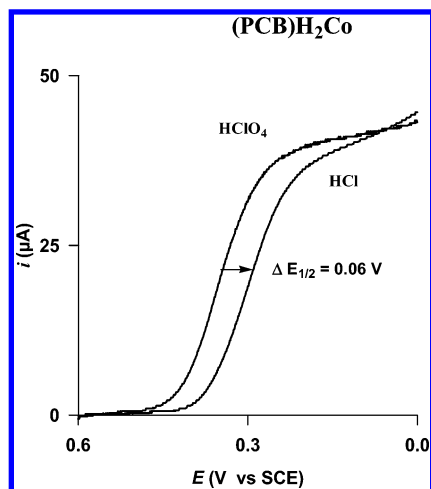
	1 M HClO$_4$			1 M HCl		
compound	$E_p{}^a$	$E_{1/2}{}^b$	n^c	$E_p{}^a$	$E_{1/2}{}^b$	$\Delta E_{1/2}$ (HClO$_4$−HCl)
(PCA)H$_2$Co	0.30	0.35	2.8	0.21	0.28	0.07
(PCX)H$_2$Co	0.31	0.35	2.5	0.23	0.28	0.07
(PCB)H$_2$Co	0.29	0.35	2.9	0.24	0.29	0.06
(Me$_4$Ph$_5$Cor)Co	0.36^d	0.38^d	2.9^d	0.28	0.33	0.05

^{a} Peak potential of the dioxygen reduction wave (V vs SCE). ^{b} Half-wave potential (V vs SCE) for dioxygen reduction at a rotating disk electrode ($\omega = 100$ rpm). ^{c} The apparent number of electrons transferred per dioxygen molecule (*n*) at $E_{1/2}$ is calculated from $n = 4I_D/(I_D + I_R/N)$ where I_D and I_R are disk and ring currents, respectively, and N (= 0.24) is the collection efficiency of the ring-disk electrode. ^{d} Data taken from ref 8.

Figure 8. Reduction of O_2 at a rotating disk electrode coated with (PCB)-H_2Co in air-saturated 1 M $HClO_4$ or 1 M HCl. Rotating rate: 100 rpm. Scan rate: 5 mV/s.

Catalytic Reduction of O_2 in 1 M HCl. The catalytic reduction of dioxygen by (PCY)H_2Co and the monocorrole, (Me$_4$Ph$_5$Cor)Co, was also investigated by cyclic voltammetry and rotating disk electrode voltammetry in 1 M HCl, where Cl^- from the acid would be expected to coordinate to the Co(IV) center of the corrole adsorbed on the electrode surface. As shown in Figure 8, the electrocatalytic reduction wave of dioxygen recorded in air-saturated 1 M HCl at a graphite disk coated with (PCB)H_2Co is shifted by 60 mV toward more negative potentials, consistent with Cl^- coordinating to the Co(IV) center of the porphyrin−corrole dyad. A similar negative shift is seen for the other two (PCY)H_2Co complexes as well as for (Me$_4$Ph$_5$Cor)Co in HCl, and the magnitude of the shift in $E_{1/2}$ is listed in Table 4 as $\Delta E_{1/2}$, which ranges from 50 to 70 mV. The fact that (PCY)H_2Co and (Me$_4$Ph$_5$Cor)Co both catalyze the reduction of dioxygen in the presence of Cl^- (see Table 4) suggests that the anionic axial ligand is rapidly released when the cobalt(IV) center is reduced to Co(III) in the dyad.

Summary. A strong binding of Cl^- to the corrole cobalt center is shown to occur for all of the Co(IV) derivatives as well as for the doubly charged Co(IV) π-cation radical of (PCA)H_2Co and (Me$_4$Ph$_5$Cor)Co in nonaqueous media. The Co(III) monocorrole in its neutral form also binds a single Cl^- axial ligand in PhCN, but Cl^- binding by Co(III) or Co(II) does not occur for any of the three investigated dyads under the same solution conditions. The $E_{1/2}$ for electrocatalysis of O_2 in $HClO_4$ and HCl parallels changes in potential for the Co(IV)/Co(III) reaction of the dyads adsorbed on a graphite electrode. The half-wave potential for electrocatalysis also shifts negatively upon going from 1 M $HClO_4$ to 1 M HCl, and this is consistent with the binding of Cl^- to the electrooxidized Co(IV) center of the adsorbed corrole.

Although the electrocatalytic reduction of O_2 by the (PCY)H_2Co dyads is not enhanced by the binding of Cl^-, the large formation constants for the addition of Cl^- to the neutral and electrooxidized forms of (Me$_4$Ph$_5$Cor)Co in CH_2Cl_2 or PhCN suggest the possibly that the investigated monocorrole and related porphyrin−corrole dyads might find application in the area of sensors and anion recognition, as has earlier been explored in the case of porphyrins.[31−34] The binding of other anions to Co(III) and Co(IV) corrole centers is also possible, and studies of these ligand binding reactions are now in progress.

Supporting Information Available: Additional figures (Figures S1 and S2). Figure S1 illustrates the UV−visible spectra of (Me$_4$-Ph$_5$Cor)Co^{III}(CO) in CH_2Cl_2 and [(Me$_4$Ph$_5$Cor)Co^{III}Cl]$^-$ in PhCN, and Figure S2 shows cyclic voltammograms of (PCB)H_2Co in PhCN and 0.1 M TBAP with 0−160 equiv of TBACl. This material is available free of charge via the Internet at http://pubs.acs.org.

IC050738N

(31) (a) Górski, L.; Malinowska, E.; Parzuchowski, P.; Zhang, W.; Meyerhoff, M. E. *Electroanalysis* **2003**, *15*, 15−16. (b) Steinle, E. D.; Schaller, U.; Meyerhoff, M. E. *Anal. Sci.* **1998**, *14*, 79−84.
(32) Jagessar, R. C.; Shang, M.; Scheidt, W. R.; Burns, D. *J. Am. Chem. Soc.* **1998**, *120*, 11684−11692.
(33) Kano, K.; Kitagidhi, H.; Tamura, S.; Yamada, A. *J. Am. Chem. Soc.* **2004**, *126*, 15202−15210.
(34) Badr, I. H. A.; Meyerhoff, M. E. *J. Am. Chem. Soc.* **2005**, *127*, 5318−5319.